Identification of Landslide-prone Zones Using a GIS-based Multi-Criteria Decision Analysis and Region Growing Algorithm in Uncertain Conditions

sara beheshtifar (sara_beheshtifar@yahoo.com)
University of Tabriz https://orcid.org/0000-0003-0044-6101

Research Article

Keywords: Landslide-prone zones mapping, Interval comparison matrix (ICM), Analytical hierarchy process (AHP), interval number distance based region growing (IDRG), Urmia lake basin

Posted Date: December 15th, 2021

DOI: https://doi.org/10.21203/rs.3.rs-1099128/v1

Identification of Landslide-prone Zones Using a GIS-based Multi-Criteria Decision Analysis and Region Growing Algorithm in Uncertain Conditions

Sara Beheshtifar, Ph.D.,
Assistant Professor, Surveying and Geomatics Eng. Department, Faculty of Civil Engineering,
University of Tabriz, 29 Bahman Blvd., Tabriz, Iran.
E-mail: sara_beheshtifar@yahoo.com

Abstract

Landslides are considered to be one of the most significant natural hazards. Detection of landslide-prone zones is an important phase in landslide hazard assessment and mitigation of landslide-related losses. AHP as one of the most effective methods for GIS-based multi-criteria decision analysis is increasingly being used in susceptibility mapping. However, its weights have some degree of uncertainty that interval comparison matrix (ICM) method can be used to deal with this problem. The importance of this study is to propose an interval number distance-based region growing (IDRG) method based on ICM for the identification of landslide-prone zones in the Urmia lake basin, Iran. To assess the capability of the proposed IDRG method, a landslide susceptibility map was produced using common AHP, too. To generate the maps, the weights of nine conditioning factors were determined using both traditional pairwise comparison matrices (PCM) of the AHP method and ICM. The accuracy of the produced maps was assessed through ROC (receiver operating curve) and using a dataset of known landslide occurrences. The results indicate an improvement in accuracy of about 11% by identifying the landslide-prone zones using the IDRG method. This improvement was achieved by minimizing the uncertainty associated with criteria ranking/weighting in a traditional AHP and identifying the prone zones as areas instead of pixels.

Keywords: Landslide-prone zones mapping, Interval comparison matrix (ICM), Analytical hierarchy process (AHP), interval number distance based region growing (IDRG), Urmia lake basin.

١. Introduction

Landslide is known as a natural hazard that often occurs in mountainous and hilly areas all over the world (Akgun & Erkan, 2016). Landslide is a type of mass movement, and it is the rapid fall of the large volume of rocks and soils from upslope to downslope (Chorley, 1985; Malamud, Turcotte, Guzzetti, & Reichenbach, 2004). Landslides commonly lead to loss of human life and property, as well as causing critical damage to natural resources (Bakhtiar Feizizadeh & Blaschke, 2013). Landslide evaluations can reduce the hazard to a certain level by producing hazard zonation maps (X. Chen & Chen, 2021). Such maps would facilitate the discovery of susceptible areas and manage regional land use (Mohammady, Pourghasemi, & Pradhan, 2012). So far, landslide susceptibility has been analyzed utilizing GIS together with diverse models like frequency ratio (FR) (Aditian, Kubota, & Shinohara, 2018; Ding, Chen, & Hong, 2017; Khan et al., 2019; Kumar & Anbalagan, 2015; Zhang et al., 2016), analytical hierarchical process (AHP) (Althuwaynee, Pradhan, Park, & Lee, 2014; Bahrami, Hassani, & Maghsoudi, 2021; He, Hu, Sun, Zhu, & Liu, 2019; Myronidis, Papageorgiou, & Theophanous, 2016; Shahabi, Khezri, Ahmad, & Hashim, 2014), analytical network process (ANP) (Abedi Gheshlaghi & Feizizadeh, 2017; Alizadeh, Ngah, Hashim, Pradhan, & Pour, 2018), support vector machines (SVM) (Ada & San, 2018; Y. Huang & Zhao, 2018; Pham, Jaafari, Prakash, & Bui, 2019; Z. Wang & Brenning, 2021; Xing et al., 2021), random forest (RF) (Nhu et al., 2020; Sun, Wen, Wang, & Xu, 2020), evidence belief function (EBF) (Althuwaynee et al., 2014; Z. Chen, Liang, Ke, Yang, & Zhao, 2020; Ding et al., 2017; Feby, Achu, Jimnisha, Ayisha, & Reghunath, 2020; Zhang et al., 2016), Dempster–Shafer (W. Chen, Pourghasemi, & Zhao, 2017; Bakhtiar Feizizadeh & Blaschke, 2014; Bakhtiar Feizizadeh, Jankowski, & Blaschke, 2014; Gudiyangada Nachappa, Tavakkoli Piralilou, Ghorbanzadeh, Shahabi, & Blaschke, 2019; Hosseinpoor Milaghardan, Ali Abbaspour, & Khalesian, 2020; Mezaal, Pradhan, & Rizeei, 2018; Mohammady et al., 2012; Pourghasemi, Pradhan, Gokceoglu, & Moezzi, 2013; Shirani, Pasandi, & Arabameri, 2018), decision tree (Wang et al., 2016; Pham, et al. 2020, Wu, et al. 2020), logistic regression (LR) (Aditian et al., 2018; Althuwaynee et al., 2014; Felicísimo, Cuartero, Remondo, & Quirós, 2013; Pradhan et al., 2008; L.-J. Wang, Guo, Sawada, Lin, & Zhang, 2016),, fuzzy logic (Feizizadeh et al. 2014, Kumar and Anbalagan 2015, Abedi Gheshlaghi and Feizizadeh 2017, Bahrami et al. 2021), artificial neural networks (Gorsevski et al., 2016; Wang et al., 2016; Aditian et al., 2018), and deep learning algorithms (Bui et al. 2020, Dao et al. 2020, Huang et al. 2020, Nhu, Hoang, et al. 2020, Thi Ngo et al. 2021). All the methods have their particular advantages and disadvantages, and each model's functioning varies based on the input data, the structure of the model, and the accuracy of the model (Nachappa, Ghorbanzadeh, Gholamnia, & Blaschke, 2020). However, there is no suggestion that a particular model must be utilized for a specific situation or study area. The analytical hierarchy process (AHP) with the aim of GIS is one of the most effective methods for assessing the landslide susceptibility of the area (Althuwaynee et al., 2014; Shahabi et al, 2014; Myronidis et al., 2016; He et al., 2019; Bahrami et al, 2021). The conventional AHP method uses exact experts 'judgments structured in a pairwise comparison matrix (PCM) by applying Saaty's scale of importance amounts (scale of 1 to 9) (Boroushaki & Malczewski, 2008; Saaty, 2008). The relative importance of different conditioning factors is determined as crisp values based on the PCM (Lan, Lin, & Cao, 2009). Despite the advantages of the

AHP, the uncertainty of weights lies in the subjective expert judgment may have meaningful impacts on the results, which may sometimes lead to inaccurate outcomes (H. Chen, Wood, Linstead, & Maltby, 2011; Bakhtiar Feizizadeh, Jankowski, et al., 2014; Lan et al., 2009). Several methods have been applied to reduce the amount of uncertainty associated with the AHP method, such as the application of fuzzy logic, interval comparisons, and spatial sensitivity analysis (Boroushaki & Malczewski, 2008; Y. Chen, Yu, & Khan, 2013; Bakhtiar Feizizadeh & Blaschke, 2014; Bakhtiar Feizizadeh, Shadman Roodposhti, Jankowski, & Blaschke, 2014). Due to the complexity involved in real-world decision problems, it is easier for a decision-maker to provide an interval comparison matrix and derive the interval weights than crisp ones (Cabrera-Barona & Ghorbanzadeh, 2018; Entani & Tanaka, 2007; Bakhtiar Feizizadeh & Ghorbanzadeh, 2017; Lan et al., 2009). On the other hand, most of the previous researches applied the pixel-based classification to produce the final susceptibility landslide map (Feby et al., 2020; Bakhtiar Feizizadeh & Blaschke, 2013; B. Feizizadeh, Blaschke, Nazmfar, & Rezaei Moghaddam, 2013). Using this method may lead to the classification of a single pixel in a particular class (e.g. very high-risk) which is surrounded by the pixels of the other classes, whereas in reality this rarely happens. In this study, a region-based method is applied to determine landslide-prone zones, instead of a pixel-based method. The region-based classification includes the segmentation of neighboring pixels into homogenous units or objects. Object-oriented methods have become more popular for image classification in recent years (Trang et al., 2016), but they haven't been applied for the classification of susceptibility maps.

The main objective of this study was to develop a new approach to determine landslide-prone zones as regions based on the concept of interval numbers for tackling uncertainty within the weights of criteria in the AHP method. The second objective was to produce landslide susceptibility maps for the study area. The third objective was to compare the accuracy of the proposed model with the common AHP method. All the analyses were performed using Matlab and ArcGIS software. In following these objectives, we developed a new interval number distance-based region growing (IDRG) method. This new technique was then tested for landslide susceptibility mapping (LSM) in the Urmia lake basin, Iran.

۲. Study area and data

The study area is the Urmia lake basin, which is located in the northwest of Iran (see Figure 1). The size of the study area is 19,913 km2 and its elevation is between 1260 m to 3710 m above sea level. The climate of this area is semi-arid and the annual precipitation is about 300 mm. The complexity of the geological structure in the related lithological units in the Urmia Lake basin has played an important role in the occurrence of numerous landslides in the region (Bakhtiar Feizizadeh & Blaschke, 2013). A landslide inventory atabase for the East Azerbaijan Province lists 132 known landslide events. In this study, based on fieldwork and expert knowledge, nine conditioning factors were selected including Aspect, Distance to roads, Elevation, Distance to stream, Distance to faults, Slope, Land-use, Precipitation, and Lithology. After that, all datasets were prepared and arranged in ArcGIS software as raster maps with a resolution of 100 m for further analysis.

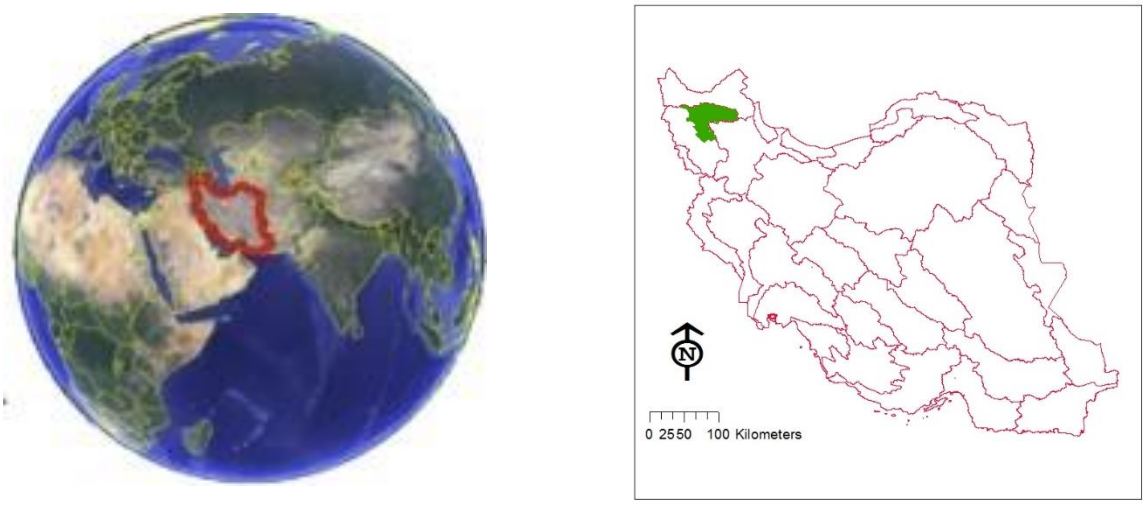

Fig. 1. Study area: Iran, Urmia lake basin

٣. Methodology

In this study, a region growing method is proposed based on interval number distance to determine the landslide-prone zones. The input map includes pixels with interval values which are determined using ICM based on the AHP method. The results were compared with the common AHP method (see Figure 2).

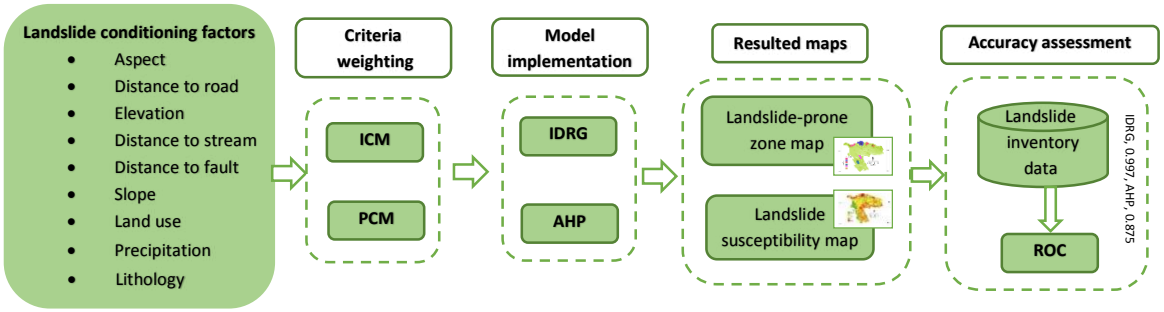

Figure 2. The methodological framework

٣٠١. Region growing

The Seeded Region Growing (SRG) is a segmentation method that checks adjacent pixels of initial seed points and determines whether the pixel neighbors should be added to the region depending on a similarity criterion (Adams & Bischof, 1994; Z. Huang, Wang, Wang, Liu, & Wang, 2018). Seed points are usually selected based on some user criterion such as pixels in a certain intensity or grayscale range.

٣٠٢. Interval Analytic Hierarchy Process (IAHP)

The Analytic Hierarchy Process (AHP) is a popular method for solving multi-criteria decision-making problems. The conventional AHP needs exact judgments and forms crisp comparison matrices to explicit the preference information (Wei, Huang, & Zhang, 2008). However, the inherent subjective nature of expert judgments is a source of significant uncertainty in the AHP method. To overcome this problem, it is better

to arrange an interval comparison matrix for deriving the weights (Bakhtiar Feizizadeh & Ghorbanzadeh, 2017). In this method, the decision-maker offers his interval judgments $x_{ij}=[l_{ij},u_{ij}]$, instead of a crisp number, where x_{ij} indicates that the alternative x_i is between l_{ij} and u_{ij} times as important as the alternative x_j, then an interval comparison matrix (ICM) **A** can be structured as (Lan et al., 2009):

$$A=\begin{bmatrix} 1 & [l_{12}\ u_{12}] & \cdots & [l_{1n}\ u_{1n}] \\ \vdots & & \ddots & \vdots \\ [l_{n1}\ u_{n1}] & & \cdots & 1 \end{bmatrix} \quad (1)$$

$l_{ij}\leq u_{ij}, \quad \forall i,j=1,2,\ldots,n$ and $l_{ij}\geq 0$, $u_{ij}\geq 0, \quad \forall i,j=1,2,\ldots,n$

This matrix is a reciprocal matrix as well as a definite comparison matrix. It is defined as:

$$l_{ij}=\frac{1}{u_{ji}}, \quad u_{ij}=\frac{1}{l_{ji}}, \quad \forall\ i,j=1,2,\ldots,n \quad (2)$$

The approach of generating this matrix and deriving the interval weights is explained in detail by Liu (2009) and Ghorbanzadeh et al. (2018). The ICM of this study is shown in Table 1.

Table 1 Interval pairwise comparison matrix

	1	2	3	4	5	6	7	8	9
(1)Aspect	1								
(2) Distance to road	[2 3]	1							
(3) Elevation	[1/3 1/2]	[1/4 ½]	1						
(4) Distance to stream	[1 2]	[2 4]	[3 4]	1					
(5) Distance to fault	[1 2]	[2 3]	[1 2]	[2 3]	1				
(6) Slope	[6 8]	[4 6]	[8 9]	[2 4]	[3 5]	1			
(7) Land use	[7 9]	[5 7]	[3 4]	[3 6]	[2 4]	[2 4]	1		
(8) Precipitation	[8 9]	[6 7]	[7 8]	[7 8]	[3 6]	[2 3]	[4 6]	1	
(9) Lithology	[8 9]	[7 8]	[2 3]	[7 8]	[7 8]	[3 5]	[4 6]	[8 9]	1

The final interval weight matrix W was calculated according to the ICM using the method proposed by Liu (2009) and then normalized (Table 2).

Table 2 Interval weights of criteria

Criterion	**Weight**	**Criterion**	**Weight**
(1)Aspect	[0.0530 0.0737]	(6) Slope	[0.2776 0.2850]
(2) Distance to road	[0.0662 0.0866]	(7) Land use	[0.2878 0.3579]
(3) Elevation	[0.0502 0.0548]	(8) Precipitation	[0.4569 0.5713]
(4) Distance to stream	[0.0975 0.1018]	(9) Lithology	[0.8132 1.0000]
(5) Distance to fault	[0.1087 0.1147]		

In this study, unlike the previous studies, the interval weights were calculated for sub-criteria, too (Table 3).

Table 3 Interval weights of sub-criteria

Criteria	Weight	Criterion	Weight
Distance to road (m)		**Slope (%)**	
0-100	[0.2245 0.2347]	0–10	[0.0655 0.2164]
100-200	[0.1969 0.2116]	10.1–20	[0.1638 0.1953]
200-300	[0.1800 0.1985]	20.1–30	[0.4639 0.5405]
300-500	[0.1282 0.1922]	30.1–40	[0.2164 0.3563]
>500	[0.0472 0.1006]	> 40.1	[0.0441 0.0907]
Distance to stream (m)		**Aspect**	
0–50	[0.4983 0.7577]	Flat	[0.0428 0.0623]
51–100	[0.2069 0.3363]	North	[0.0700 0.0755]
101–150	[0.1675 0.1883]	East	[0.1229 0.1474]
151–200	[0.0927 0.1132]	West	[0.3902 0.4498]
>200	[0.0471 0.0856]	Sought	[0.7738 1.0000]
Distance to fault (m)		**Land use**	
0–1000	[0.4440 0.8059]	Settlement	[0.0342 0.0525]
1001–2000	[0.2378 0.3216]	Orchard and croplands	[0.0571 0.0675]
2001–3000	[0.1006 0.1148]	Dry-Farming & pasture lands	[0.2435 0.2886]
3001–4000	[0.0975 0.2487]	Bare soil	[0.4158 0.4639]
>4000	[0.0645 0.0711]	Rock bodies	[0.4639 0.7923]
Elevation		**Lithology**	
1260–1400	[0.0310 0.0364]	Altered zone	[0.0483 0.0856]
1401–1800	[0.3957 0.4164]	Metamorphic-Plutonic	[0.0800 0.0949]
1801–2500	[0.7534 0.8704]	Plutonic	[0.1443 0.1443]
2501–3000	[0.1659 0.2032]	Volcanic	[0.3774 0.4188]
3001–3680	[0.0800 0.1043]	Metamorphic-volcanic	[0.4246 0.7981]
Precipitation			
< 250	[0.0618 0.1131]		
251–300	[0.1670 0.2270]		
301–350	[0.2270 0.5612]		

According to table 3, for each of the conditioning factors, two maps were generated, the first map was produced based on the lower bound of the interval weight and the second one was made by the upper bound of the interval weight (Figure 3).

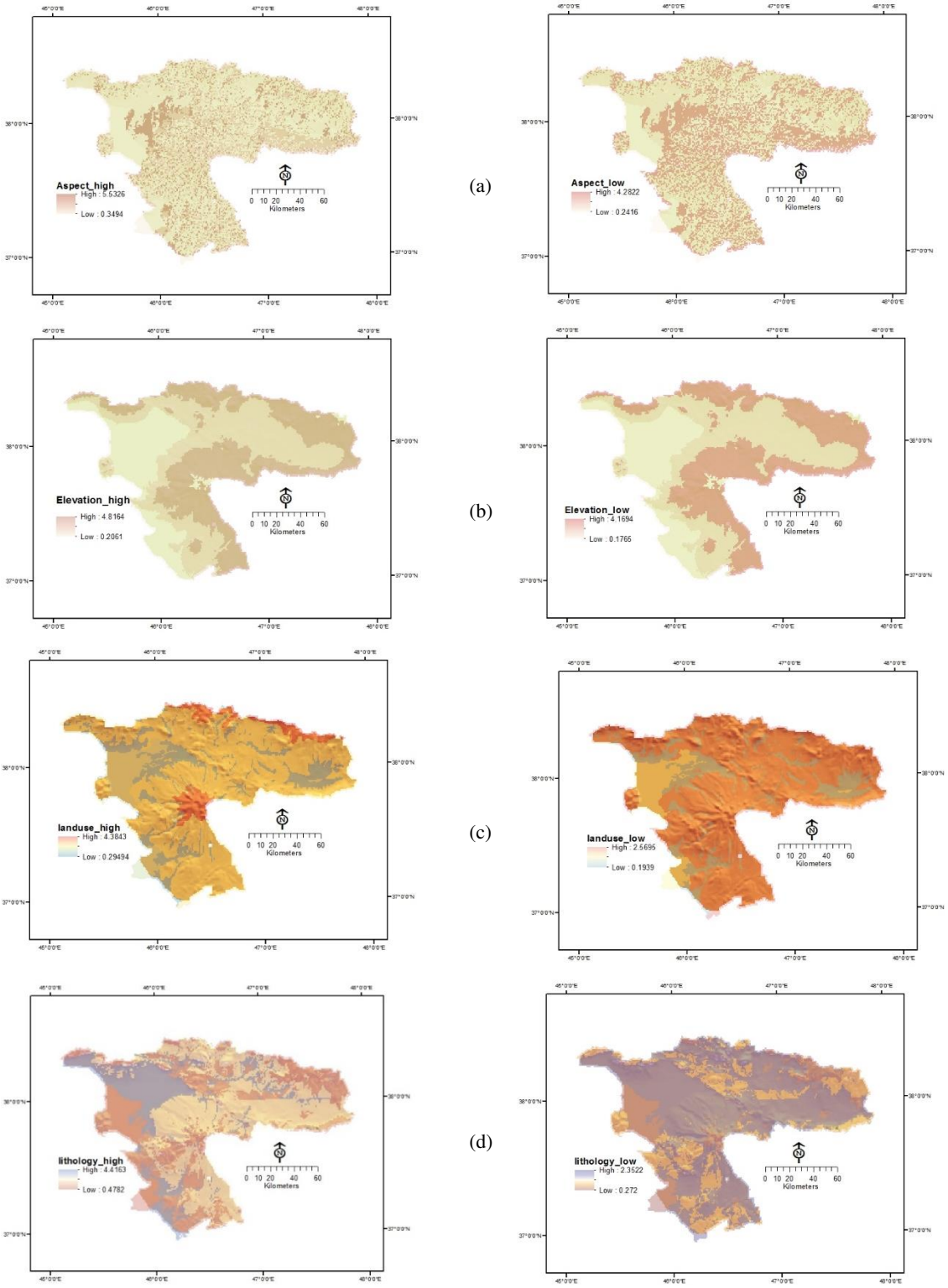

Figure 3. Landslide conditioning factors based on upper bound (left) and lower bound (right) of sub-criteria: (a) aspect, (b) elevation, (c) land use, (d) lithology, …

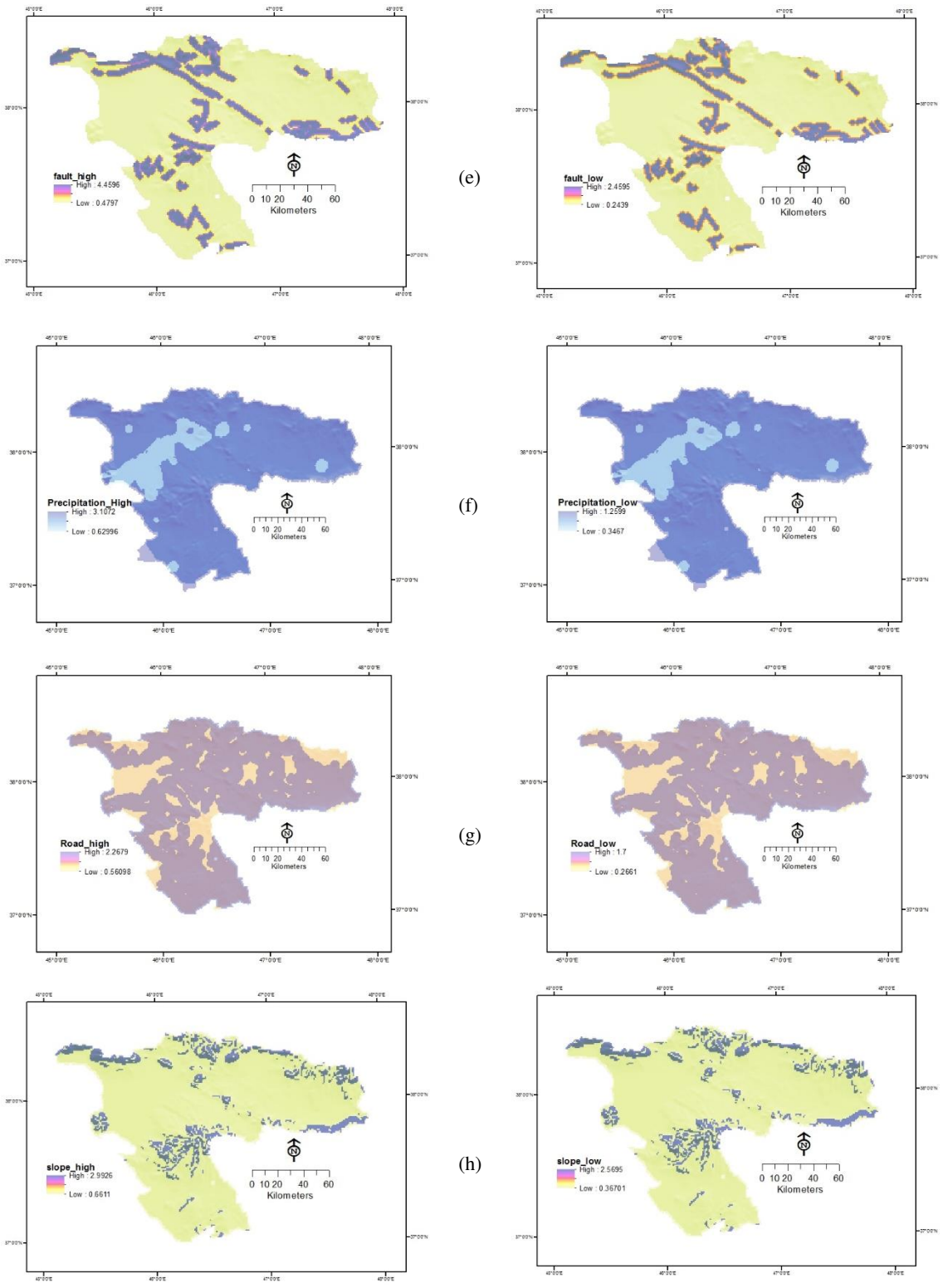

Figure 3. (con) Landslide conditioning factors based on upper bound (left) and lower bound (right) of sub-criteria: (e) distance to faults, (f) precipitation, (g) distance to roads, (h) slope, ...

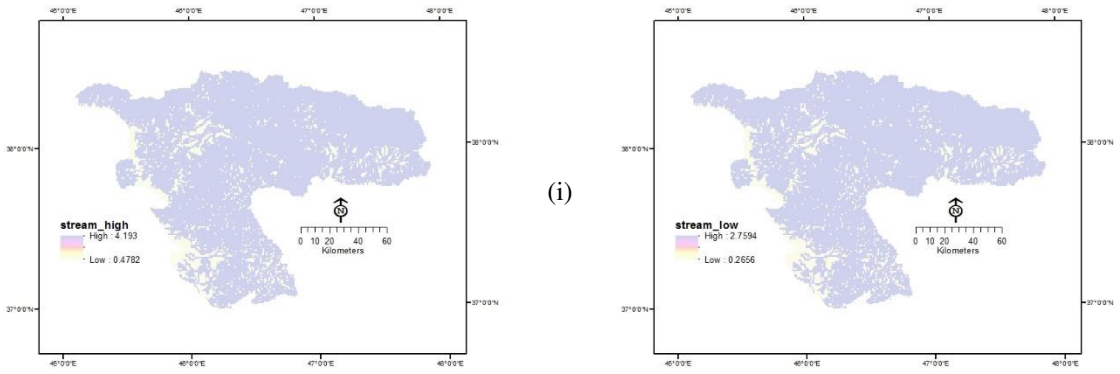

(i)

Figure 3. (con) Landslide conditioning factors based on upper bound (left) and lower bound (right) of sub-criteria: (i) distance to streams

After that, the weight of all conditioning factors (criteria) was multiplied by the related map concerning the definition of the binary operations for interval numbers as follows:

Let x=$[\underline{x}, \overline{x}]$ and y=$[\underline{y}, \overline{y}]$ be real intervals. The binary operations addition (+), subtraction (-), multiplication (.), and division (/) are then defined on R as follows:

- $x + y=[\underline{x} + \underline{y}, \overline{x} + \overline{y}]$
- $x - y=[\underline{x} + \underline{y}, \overline{x} - \overline{y}]$
- $x.\ y=[\min\{\underline{x}.\ \underline{y}, \underline{x}.\ \overline{y}, \overline{x}.\ \underline{y}, \overline{x}\ , \overline{y}\}\ , \max\ \{\underline{x}.\ \underline{y}, \underline{x}.\ \overline{y}, \overline{x}.\ \underline{y}, \overline{x}\ , \overline{y}\}]$
- $\frac{x}{y}=x.y'$, where $y' = [\frac{1}{\overline{y}}, \frac{1}{\underline{y}}]$ and y$\notin$ 0

In this step, all the conditioning factor maps were added together concerning the definition of the sum operator for interval numbers. Now we have a susceptibility map in which, each pixel includes an interval value.

۳۰۳. Interval value Distance

Let $\bar{a} = [a^-, a^+]$ and $\bar{b} = [b^-, b^+]$ be two interval numbers. Yu (2013) proposed an IND[1]definition based on the median and width of the interval number (Guo et al., 2018, Yu 2013).

$$\tilde{d}_{EW}(\bar{a}, \bar{b})=\sqrt[P]{\left|E(\bar{a}) - E(\bar{b})\right|^P + \frac{1}{2}\left|W(\bar{a}) - W(\bar{b})\right|^P} \quad ,p\geq 1$$

where $E(\bar{a}) = \frac{a^- + a^+}{2}$ is the median of $\bar{a}$ and $W(\bar{a})= \frac{a^- - a^+}{2}$ is the width of $\bar{a}$.

۳۰۴. Interval number Distance based Region Growing (IDRG) (A novel approach)

In this study, a new method was proposed to identify homogenous regions using interval values: Interval number Distance based Region Growing (IDRG). The algorithm classifies each pixel of the map as regions (e.g. high-risk zones) or backgrounds. In the proposed algorithm, it is assumed that the values of pixels in the input map are represented by interval numbers, in which the width of interval numbers are related to the uncertainty of the values (The lower interval width for a pixel value shows the lower uncertainty).

Two main concerns should be dealt with when executing a region growing algorithm: where to place the initial seeds and which similarity criterion should be assumed to characterize the regions (Z. Huang et al.,

[1] Interval number distance

2018). The most common way is to select some pixels as seed points based on simple criteria (e.g. color, intensity, or texture). In the input map, the value and the position of pixels by higher median and lower width can be determined. In IDRG, it is proposed to select them as seed points to avoid false detections and to focus on the segmentation itself.

The similarity criterion was defined to identify regions within which there is similarity and uniformity in both quantity and uncertainty. To specify the similarity criterion, the interval distance between the region's mean and a new neighbor pixel is calculated based on the IND definition proposed by Yu (2013). At the first step, each seed is considered as a region, and IND is calculated between seed points and their neighbors. In cases that the smallest IND between the mean of the region and the new pixel becomes lower than a certain threshold (t), the pixel joins to the region, and the region is iteratively grown. At the next steps, the region's mean is calculated according to all pixels of the segmented region. In the end, the pixels that have three or four adjacent pixels belong to one region, joining the same region. The proposed IDRG is as follows:

Algorithm: Interval number Distance based Region Growing procedure

E: Map of Median (Calculated using interval pixel values)
W: Map of Width (Calculated using interval pixel values)
R: logical map of regions
X, Y: the position of the seed points (determined based on E and W)
t: maximum Interval number distance (IND)
Input: *E, W, X, Y, t*
Output: *R*
1: R= seed point
2: Reg_mean=E (X, Y)
3: Reg_width=W (X, Y)
4: N_i= Neighbor of R
5: ***if*** *IND (R (Reg_mean, Reg_width), N_i (E, W)) $<t$ then*
$R=R \cup N_i$
Reg_mean=mean(R(E))
Reg_width= mean(R(W))
6: ***Endif***
7: ***Repeat*** *(from step 4)*

٤. Landslide-prone zone map generation using IDRG algorithm

In this case study, after initial processes, the weightings derived from ICM were used for data aggregation within a GIS environment. Two aggregated maps were generated, the first one indicates the lower bound and the second one shows the upper bound. The first map was produced using the lower bound map of the conditioning factors (fig 3. Left) and lower weight of the criteria. The second map was generated using the upper bound map of the conditioning factors (fig 3. Right) and upper weight of the criteria. These maps were imported into the Matlab environment and a new map was produced by interval numbers in which the width of interval numbers is related to the weights of IAHP. This map was considered as the input of IDRG. Moreover, according to the interval value of pixels, median map (E) and width map (W) were produced (Figure 4). The value and the position of pixels that are related to the highest risk (higher median) and least

uncertainty (lower width) can be determined. These pixels were selected as seed points for IDRG (Figure 4).

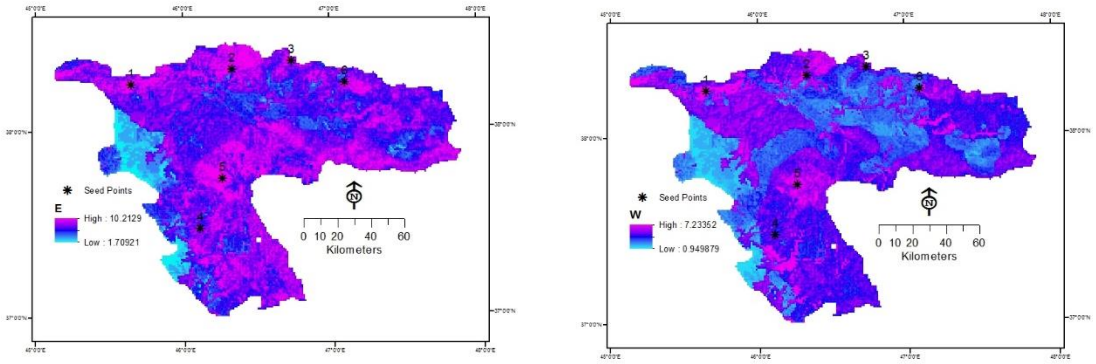

Figure 4. Seeds on produced maps by median (left) and width (right) of internal numbers

Then, landslide-prone regions were identified for each seed according to the similarity criteria using the IDRG procedure. In this work, 4-connected neighborhoods for seed pixels were checked to determine whether the pixel neighbors should be added to the region. The region is iteratively grown by comparing unallocated neighboring pixels to the region. The pixel with the smallest IND measured this way is allocated to the respective region. This process stops when the IND between the mean of the region and the new pixel becomes larger than a certain threshold (t). After that, in our proposed method, to create homogenous regions, if three or four neighbors of a pixel belonging to a region, that pixel itself join that region. These regions were then exported from the MATLAB programming environment into the ArcGIS 10.3 software. Then, the regions were converted into a landslide-prone zone map.

۵. Landslide susceptibility map generation using conventional AHP method

To compare the results of the proposed IDRG method with the conventional AHP, a landslide susceptibility map was produced using the same conditioning factors and AHP. The weights of criteria and sub-criteria were calculated based on eigenvalues using a conventional pairwise comparison matrix (PCM) proposed by Saaty (2008). The weights are resented in Table 3 (Feizizadeh and Blaschke, 2013).

Table 3 Weights of criteria and sub-criteria in conventional AHP

Criteria	Weight	Criteria	Weight	Criteria	Weight
Distance to road (m)	**0.036**	**Slope (%)**	**0.141**	**Elevation**	**0.02**
0-100	0.269	0–10	0.09	1260–1400	0.076
100-200	0.255	10.1–20	0.18	1401–1800	0.239
200-300	0.249	20.1–30	0.47	1801–2500	0.393
300-500	0.135	30.1–40	0.15	2501–3000	0.173
>500	0.092	> 40.1	0.11	3001–3680	0.119
Distance to stream (m)	**0.112**	**Aspect**	**0.025**	**Precipitation**	**0.172**
0–50	0.51	Flat	0.046	< 250	0.17
51–100	0.21	North	0.059	251–300	0.32
101–150	0.11	East	0.109	301–350	0.51
151–200	0.091	West	0.269	**Lithology**	**0.21**
>200	0.079	Sought	0.517	Altered zone	0.09
Distance to fault (m)	**0.124**	**Land use**	**0.16**	Metamorphic-Plutonic	0.12
0–1000	0.515	Settlement	0.053	Plutonic	0.18
1001–2000	0.224	Orchard and croplands	0.067	Volcanic	0.27
2001–3000	0.126	Dry-Farming & pasture lands	0.235	Metamorphic-volcanic	0.34
3001–4000	0.085	Bare soil	0.325		
>4000	0.05	Rock bodies	0.32		

٦- Results and validation

Determined regions using the IDRG method in MATLAB environment were converted into landslide-prone zone map in ArcGIS which is shown in figure 5. After that, the area of each region was calculated (Table 4).

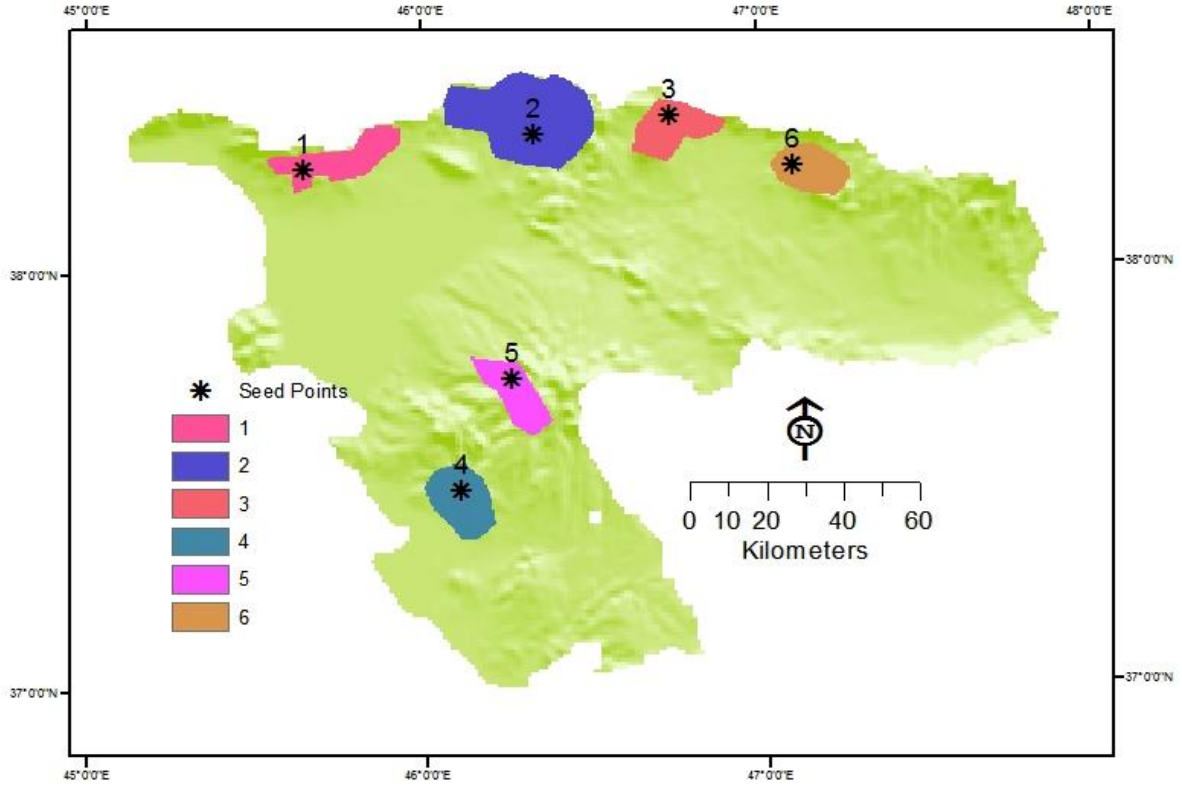

Figure 5. Landslide-prone zone map generated by IDRG method

The landslide susceptibility map generated using the conventional AHP method, was classified into five classes of susceptibility using the natural breaks classification (Jenks optimization), which is an effective method for categorizing the susceptibility maps (see fig. 6).

The accuracy of maps was evaluated based on the locations of known landslides within the study area. The validation process is a fundamental step to assess the ability of the developed approach for the identification of landslide-prone zones. The locations of observed landslides are represented on the landslide-prone zone map generated by the IDRG method in Fig. 7. The area of each region determined by the IDRG method and the number of observed landslide events are presented in Table 4.

To compare the accuracy of IDRG and conventional AHP method, the area of each category using AHP and the number of observed landslide events were determined and represented in Table 5.

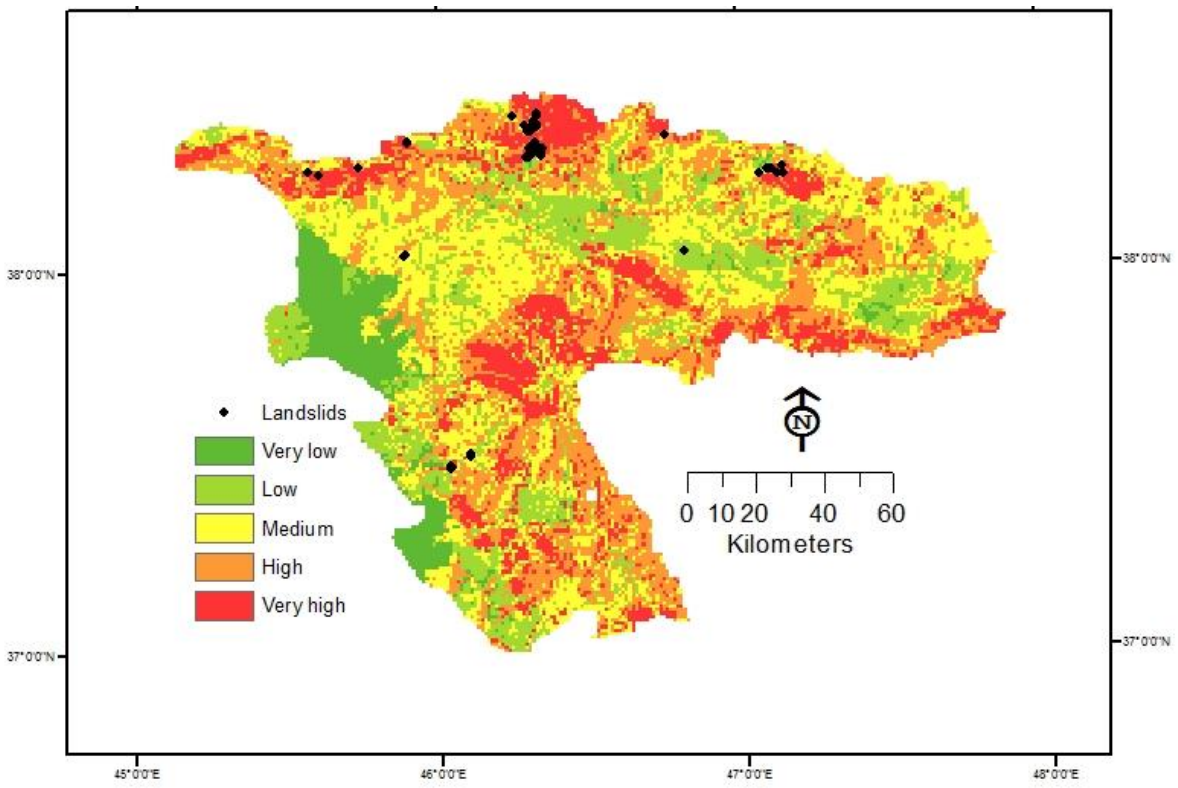

Figure ٦. Landslide susceptibility map generated by conventional AHP method

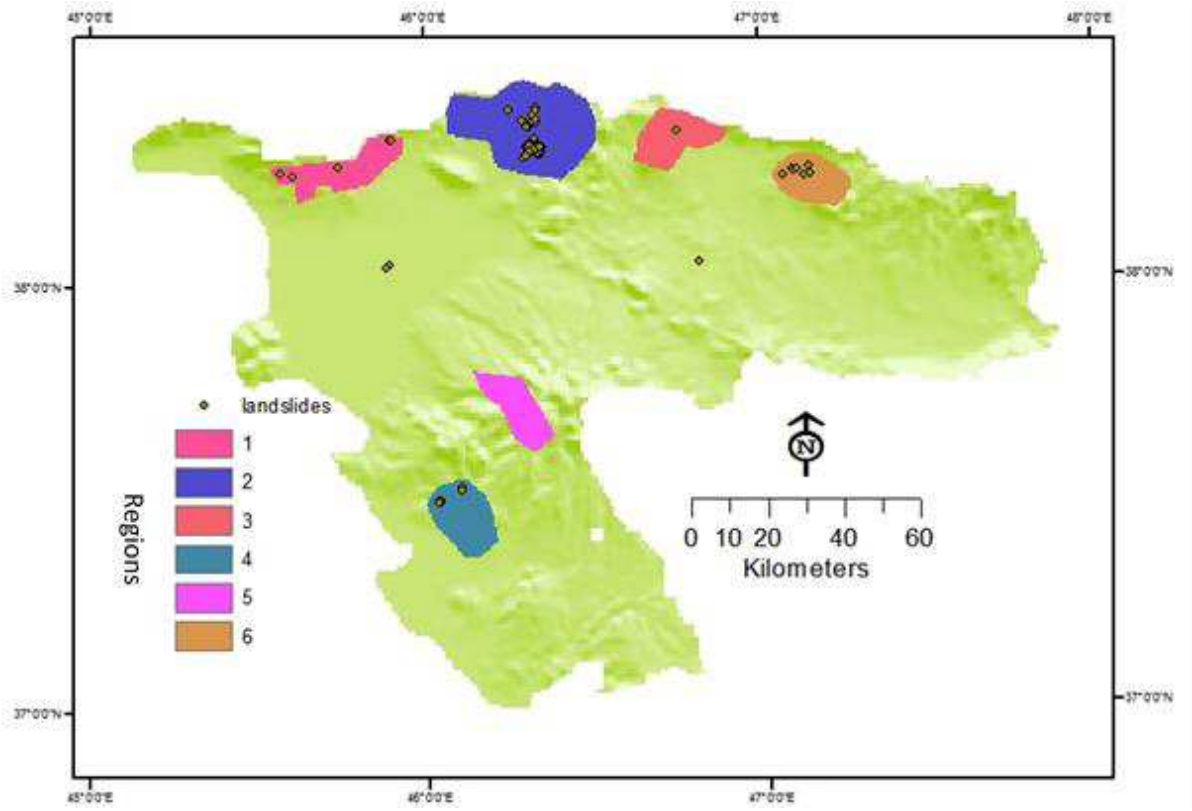

Figure 7. Observed landslides on landslide-prone zone map generated by IDRG method

Table 4 Area of each region (in IDRG method) and the number of observed landslide events

Region	Area (km2)	Percent of study area (%)	Observed Landslides	Observed Landslides (%)
1	261.11	5.66	5	3.78
2	701.63	15.19	109	82.57
3	235.56	5.09	1	0.75
4	252.16	5.46	6	4.54
5	205.92	4.46	0	0
6	181.51	3.93	8	6.06
Sum		39.79	129	97.73
Remained	2781.74	60.21	3	2.27

Table 5 Area of each category using conventional AHP and the number of observed landslide events

	Area (km2)	Percent of study area (%)	Observed Landslides	Observed Landslides (%)
Very low	340.14	37.31	0	0
Low	791.24	13.71	3	2.27
Medium	1419.29	9.79	24	18.18
High	1343.81	9.47	67	50.76
Very high	722.52	29. 72	38	28.79

According to table 5, 39.19 percent of the study area is covered by "High" and "Very high" risk classes (9.47% + 29.72%) in the susceptibility map obtained by the conventional AHP method and79.55 % of the observed landslides were located in these classes. However, the identified regions using IDRG covers 39.79 % of the study area, and 97.73 % of the known landslides were located inside the determined regions which shows the ability of the proposed method in determining the landslide-prone zones. For a more detailed

assessment of the results, a part of the region2 (adjusting pixels of seed point No. 2 in IDRG) is represented in Fig. 8. Classification of the susceptibility map based on pixels in conventional AHP may cause a single-pixel belonging to a particular class to be surrounded by pixels belonging to another class; while in reality this rarely happens. For example, as shown in Fig 8., some "Medium"-risk class pixels are surrounded by the "Very high" and "High"-class pixels. Some of the occurred landslides are observed in this area. This can be due to both considering the crisp weights for criteria and sub-criteria in the conventional AHP method and the pixel-based classification. In the proposed method, the sensitivity to the threshold value between two classes of classification is reduced and the pixels that are close in terms of value and uncertainty, are assigned to one region so that the whole area shown in Fig. 8 is inside region No. 2 in the IDRG method. Furthermore, in the proposed method, the pixels that are surrounded by pixels of a region will be joined to the region. Although it has not yet occurred any landslide in region No. 5 on the IDRG map, it is one of the high-risk areas that should be considered in decision making. In this research, the accuracies of the landslide-prone zones map produced by the IDRG method and the landslide susceptibility map generated by the conventional AHP method were evaluated by calculating relative operating characteristics (ROCs) and verifying the number of observed landslides in the various categories of the derived maps. The ROC curve is a plot of the probability of having a truly positive response (a correctly predicted event) versus the probability of a false-positive response (an incorrectly predicted event), for different probability cutoffs (Bakhtiar Feizizadeh, Shadman Roodposhti, et al., 2014; Gorsevski et al., 2016).

A landslide inventory database for the study area includes132 observed landslide events which were used to validate the results. In the ROC curve, the ideal model is denoted by a value close to 1.0 (Fawcett, 2006; Nandi & Shakoor, 2010). The results obtained from the ROC for the map derived from the IDRG method indicated an accuracy of 97% and for the map produced by conventional AHP, the accuracy was about 87% (Fig. 9). The accuracy was improved by about 10 % which shows the advantage of the IDRG method and considering the interval weights for both criteria and sub-criteria.

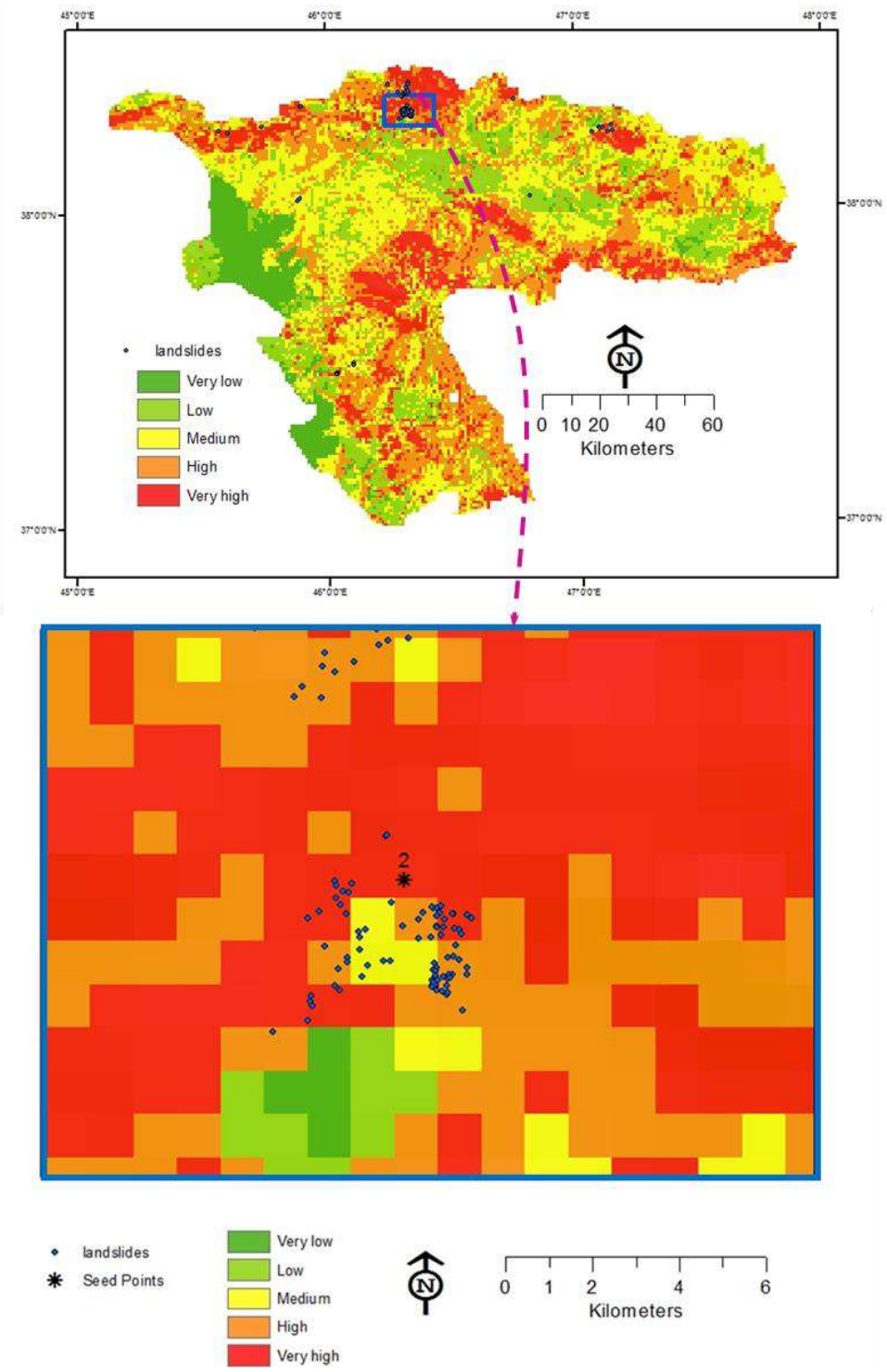

Fig 8. Neighbor pixels of seed number 2

۲۹۷

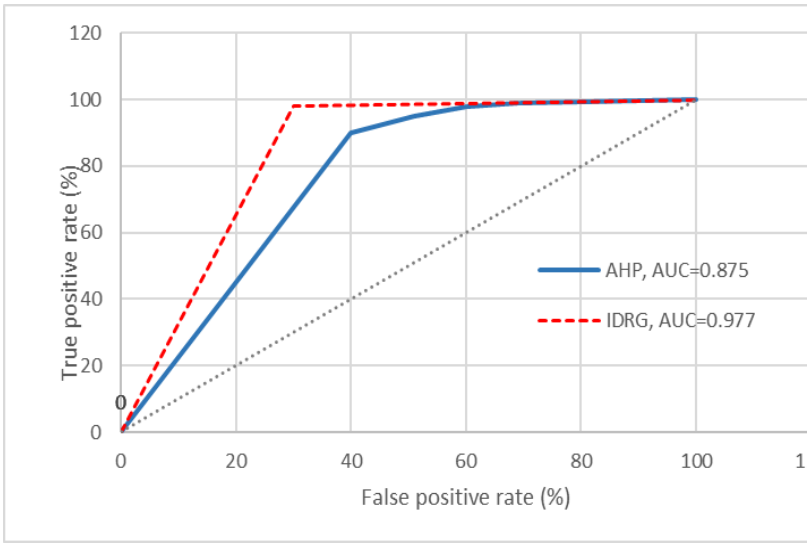

Fig. 9. Results of ROC plots for the susceptibility maps produced by IDRG and AHP methods

٦. Conclusion and future work

In this paper, we proposed a new approach that integrates the region growing algorithm with a kind of interval number distance as a measure of similarity (IDRG) to determine the landslide-prone zones in the Urmia lake basin, Iran. Using the conventional classification methods to produce landslide susceptibility maps, some sole pixels are surrounded by the pixels of the other classes, which is rarely happening in the real world. It is better to determine the landslide-prone- zones instead of high-risk pixels, as identified by the proposed IDRG method. Furthermore, the inherent uncertainty of the weights of criteria and sub-criteria determined by the experts may affect the results. Therefore, the IDRG method is proposed based on the ICM to define the weights. Using the IDRG method, 6 regions were identified as landslide-prone zones which cover 39.79 % of the study area and 97.73 % of the observed landslides were located inside them. To compare the results, a susceptibility map was produced using the conventional AHP. In this map, high and very high landslide susceptibility was detected for 39.19 % of the study area. The results achieved from the ROC, using the landslide inventory, indicated an accuracy of 97%, 87% for IDRG and conventional AHP, respectively.

By applying the proposed IDRG method to reduce the uncertainties of weights for both criteria and sub-criteria as well as determining the landslide-prone zones instead of high-risk pixels, the accuracy was improved by about 10 %.

This method can be applied to determine safe areas for decision-making in land-use planning. Furthermore, in this research to develop an interval-value-based region growing method, a binary decision map was created. However, a multi-class interval-based region growing method would be developed to support a landslide susceptibility map with multiple risk regions. Identification of Landslide-prone Zones Using a GIS-based Multi-Criteria Decision Analysis and Region Growing Algorithm in Uncertain Conditions.

References

Abedi Gheshlaghi, H., & Feizizadeh, B. (2017). An integrated approach of analytical network process and fuzzy based spatial decision making systems applied to landslide risk mapping. *Journal of African Earth Sciences, 133*, 15-24. doi:https://doi.org/10.1016/j.jafrearsci.2017.05.007

Ada, M., & San, B. T. (2018). Comparison of machine-learning techniques for landslide susceptibility mapping using two-level random sampling (2LRS) in Alakir catchment area, Antalya, Turkey. *Natural Hazards, 90*(1), 237-263. doi:10.1007/s11069-017-3043-8

Adams, R., & Bischof, L. (1994). Seeded region growing. *IEEE Transactions on pattern analysis and machine intelligence, 16*(6), 641-647.

Aditian, A., Kubota, T., & Shinohara, Y. (2018). Comparison of GIS-based landslide susceptibility models using frequency ratio, logistic regression, and artificial neural network in a tertiary region of Ambon, Indonesia. *Geomorphology, 318*, 101-111. doi:https://doi.org/10.1016/j.geomorph.2018.06.006

Akgun, A., & Erkan, O. (2016). Landslide susceptibility mapping by geographical information system-based multivariate statistical and deterministic models: in an artificial reservoir area at Northern Turkey. *Arabian Journal of Geosciences, 9*(2), 165. doi:10.1007/s12517-015-2142-7

Alizadeh, M., Ngah, I., Hashim, M., Pradhan, B., & Pour, A. B. (2018). A Hybrid Analytic Network Process and Artificial Neural Network (ANP-ANN) Model for Urban Earthquake Vulnerability Assessment. *Remote Sensing, 10*(6), 975.

Althuwaynee, O. F., Pradhan, B., Park, H.-J., & Lee, J. H. (2014). A novel ensemble bivariate statistical evidential belief function with knowledge-based analytical hierarchy process and multivariate statistical logistic regression for landslide susceptibility mapping. *CATENA, 114*, 21-36. doi:https://doi.org/10.1016/j.catena.2013.10.011

Bahrami, Y., Hassani, H., & Maghsoudi, A. (2021). Landslide susceptibility mapping using AHP and fuzzy methods in the Gilan province, Iran. *GeoJournal, 86*(4), 1797-1816. doi:10.1007/s10708-020-10162-y

Boroushaki, S., & Malczewski, J. (2008). Implementing an extension of the analytical hierarchy process using ordered weighted averaging operators with fuzzy quantifiers in ArcGIS. *Computers & Geosciences, 34*(4), 399-410. doi:https://doi.org/10.1016/j.cageo.2007.04.003

Cabrera-Barona, P., & Ghorbanzadeh, O. (2018). Comparing Classic and Interval Analytical Hierarchy Process Methodologies for Measuring Area-Level Deprivation to Analyze Health Inequalities. *International Journal of Environmental Research and Public Health, 15*(1), 140.

Chen, H., Wood, M. D., Linstead, C., & Maltby, E. (2011). Uncertainty analysis in a GIS-based multi-criteria analysis tool for river catchment management. *Environmental Modelling & Software, 26*(4), 395-405. doi:https://doi.org/10.1016/j.envsoft.2010.09.005

Chen, W., Pourghasemi, H. R., & Zhao, Z. (2017). A GIS-based comparative study of Dempster-Shafer, logistic regression and artificial neural network models for landslide susceptibility mapping. *Geocarto International, 32*(4), 367-385. doi:10.1080/10106049.2016.1140824

Chen, X., & Chen, W. (2021). GIS-based landslide susceptibility assessment using optimized hybrid machine learning methods. *CATENA, 196*, 104833. doi:https://doi.org/10.1016/j.catena.2020.104833

Chen, Y., Yu, J., & Khan, S. (2013). The spatial framework for weight sensitivity analysis in AHP-based multi-criteria decision making. *Environmental Modelling & Software, 48*, 129-140. doi:https://doi.org/10.1016/j.envsoft.2013.06.010

Chen, Z., Liang, S., Ke, Y., Yang, Z., & Zhao, H. (2020). Landslide susceptibility assessment using different slope units based on the evidential belief function model. *Geocarto International, 35*(15), 1641-1664. doi:10.1080/10106049.2019.1582716

Chorley, R. J. (1985). *Geomorphology / Richard J. Chorley, Stanley A. Schumm, David E. Sugden*. London ; New York: Methuen.

Ding, Q., Chen, W., & Hong, H. (2017). Application of frequency ratio, weights of evidence and evidential belief function models in landslide susceptibility mapping. *Geocarto International, 32*(6), 619-639. doi:10.1080/10106049.2016.1165294

Entani, T., & Tanaka, H. (2007). Interval estimations of global weights in AHP by upper approximation. *Fuzzy Sets Syst., 158*(17), 1913–1921. doi:10.1016/j.fss.2007.04.007

Fawcett, T. (2006). An introduction to ROC analysis. *Pattern Recognition Letters, 27*(8), 861-874. doi:https://doi.org/10.1016/j.patrec.2005.10.010

Feby, B., Achu, A. L., Jimnisha, K., Ayisha, V. A., & Reghunath, R. (2020). Landslide susceptibility modelling using integrated evidential belief function based logistic regression method: A study from Southern Western Ghats, India. *Remote Sensing Applications: Society and Environment, 20*, 100411. doi:https://doi.org/10.1016/j.rsase.2020.100411

Feizizadeh, B., & Blaschke, T. (2013). GIS-multicriteria decision analysis for landslide susceptibility mapping: comparing three methods for the Urmia lake basin, Iran. *Natural Hazards, 65*(3), 2105-2128. doi:10.1007/s11069-012-0463-3

Feizizadeh, B., & Blaschke, T. (2014). An uncertainty and sensitivity analysis approach for GIS-based multicriteria landslide susceptibility mapping. *International journal of geographical information science : IJGIS, 28*(3), 610-638. doi:10.1080/13658816.2013.869821

Feizizadeh, B., Blaschke, T., Nazmfar, H., & Rezaei Moghaddam, M. H. (2013). Landslide Susceptibility Mapping for the Urmia Lake basin, Iran: A multi- Criteria Evaluation Approach using GIS. *International Journal of Environmental Research, 7*(2), 319-336. doi:10.22059/ijer.2013.610

Feizizadeh, B., & Ghorbanzadeh, O. (2017). *GIS-based Interval Pairwise Comparison Matrices as a Novel Approach for Optimizing an Analytical Hierarchy Process and Multiple Criteria Weighting*.

Feizizadeh, B., Jankowski, P., & Blaschke, T. (2014). A GIS based spatially-explicit sensitivity and uncertainty analysis approach for multi-criteria decision analysis. *Computers & Geosciences, 64*, 81-95. doi:https://doi.org/10.1016/j.cageo.2013.11.009

Feizizadeh, B., Shadman Roodposhti, M., Jankowski, P., & Blaschke, T. (2014). A GIS-based extended fuzzy multi-criteria evaluation for landslide susceptibility mapping. *Computers & Geosciences, 73*, 208-221. doi:https://doi.org/10.1016/j.cageo.2014.08.001

Felicísimo, Á. M., Cuartero, A., Remondo, J., & Quirós, E. (2013). Mapping landslide susceptibility with logistic regression, multiple adaptive regression splines, classification and regression trees, and maximum entropy methods: a comparative study. *Landslides, 10*(2), 175-189. doi:10.1007/s10346-012-0320-1

Gorsevski, P. V., Brown, M. K., Panter, K., Onasch, C. M., Simic, A., & Snyder, J. (2016). Landslide detection and susceptibility mapping using LiDAR and an artificial neural network approach: a case study in the Cuyahoga Valley National Park, Ohio. *Landslides, 13*(3), 467-484. doi:10.1007/s10346-015-0587-0

Gudiyangada Nachappa, T., Tavakkoli Piralilou, S., Ghorbanzadeh, O., Shahabi, H., & Blaschke, T. (2019). Landslide Susceptibility Mapping for Austria Using Geons and Optimization with the Dempster-Shafer Theory. *Applied Sciences, 9*(24), 5393.

He, H., Hu, D., Sun, Q., Zhu, L., & Liu, Y. (2019). A Landslide Susceptibility Assessment Method Based on GIS Technology and an AHP-Weighted Information Content Method: A Case Study of Southern Anhui, China. *ISPRS International Journal of Geo-Information, 8*(6), 266.

Hosseinpoor Milaghardan, A., Ali Abbaspour, R., & Khalesian, M. (2020). Evaluation of the effects of uncertainty on the predictions of landslide occurrences using the Shannon entropy theory and Dempster–Shafer theory. *Natural Hazards, 100*(1), 49-67. doi:10.1007/s11069-019-03798-8

Huang, Y., & Zhao, L. (2018). Review on landslide susceptibility mapping using support vector machines. *CATENA, 165*, 520-529. doi:https://doi.org/10.1016/j.catena.2018.03.003

Huang, Z., Wang, X., Wang, J., Liu, W., & Wang, J. (2018). *Weakly-supervised semantic segmentation network with deep seeded region growing.* Paper presented at the Proceedings of the IEEE Conference on Computer Vision and Pattern Recognition.

Khan, H., Shafique, M., Khan, M. A., Bacha, M. A., Shah, S. U., & Calligaris, C. (2019). Landslide susceptibility assessment using Frequency Ratio, a case study of northern Pakistan. *The Egyptian Journal of Remote Sensing and Space Science, 22*(1), 11-24. doi:https://doi.org/10.1016/j.ejrs.2018.03.004

Kumar, R., & Anbalagan, R. (2015). Landslide susceptibility zonation in part of Tehri reservoir region using frequency ratio, fuzzy logic and GIS. *Journal of Earth System Science, 124*(2), 431-448. doi:10.1007/s12040-015-0536-2

Lan, J., Lin, J., & Cao, L. (2009). An information mining method for deriving weights from an interval comparison matrix. *Mathematical and Computer Modelling, 50*(3), 393-400. doi:https://doi.org/10.1016/j.mcm.2009.04.015

Malamud, B. D., Turcotte, D. L., Guzzetti, F., & Reichenbach, P. (2004). Landslide inventories and their statistical properties. *Earth Surface Processes and Landforms, 29*(6), 687-711. doi:https://doi.org/10.1002/esp.1064

Mezaal, M. R., Pradhan, B., & Rizeei, H. M. (2018). Improving Landslide Detection from Airborne Laser Scanning Data Using Optimized Dempster–Shafer. *Remote Sensing, 10*(7), 1029.

Mohammady, M., Pourghasemi, H. R., & Pradhan, B. (2012). Landslide susceptibility mapping at Golestan Province, Iran: A comparison between frequency ratio, Dempster–Shafer, and weights-of-evidence models. *Journal of Asian Earth Sciences, 61*, 221-236. doi:https://doi.org/10.1016/j.jseaes.2012.10.005

Myronidis, D., Papageorgiou, C., & Theophanous, S. (2016). Landslide susceptibility mapping based on landslide history and analytic hierarchy process (AHP). *Natural Hazards, 81*(1), 245-263. doi:10.1007/s11069-015-2075-1

Nachappa, T. G., Ghorbanzadeh, O., Gholamnia, K., & Blaschke, T. (2020). Multi-Hazard Exposure Mapping Using Machine Learning for the State of Salzburg, Austria. *Remote Sensing, 12*(17), 2757.

Nandi, A., & Shakoor, A. (2010). A GIS-based landslide susceptibility evaluation using bivariate and multivariate statistical analyses. *Engineering Geology, 110*(1), 11-20. doi:https://doi.org/10.1016/j.enggeo.2009.10.001

Nhu, V.-H., Shirzadi, A., Shahabi, H., Chen, W., Clague, J. J., Geertsema, M., . . . Lee, S. (2020). Shallow Landslide Susceptibility Mapping by Random Forest Base Classifier and Its Ensembles in a Semi-Arid Region of Iran. *Forests, 11*(4), 421.

Pham, B. T., Jaafari, A., Prakash, I., & Bui, D. T. (2019). A novel hybrid intelligent model of support vector machines and the MultiBoost ensemble for landslide susceptibility modeling. *Bulletin of Engineering Geology and the Environment, 78*(4), 2865-2886. doi:10.1007/s10064-018-1281-y

Pourghasemi, H., Pradhan, B., Gokceoglu, C., & Moezzi, K. D. (2013). A comparative assessment of prediction capabilities of Dempster–Shafer and Weights-of-evidence models in landslide susceptibility mapping using GIS. *Geomatics, Natural Hazards and Risk, 4*(2), 93-118. doi:10.1080/19475705.2012.662915

٤٣٥ Pradhan, B., Lee, S., Mansor, S., Buchroithner, M., Jamaluddin, N., & Khujaimah, Z. (2008). Utilization of optical remote sensing
٤٣٦ data and geographic information system tools for regional landslide hazard analysis by using binomial logistic regression
٤٣٧ model. *Journal of Applied Remote Sensing, 2*(1), 023542.
٤٣٨ Saaty, T. L. (2008). Decision making with the analytic hierarchy process. *International journal of services sciences, 1*(1), 83-98.
٤٣٩ Shahabi, H., Khezri, S., Ahmad, B. B., & Hashim, M. (2014). RETRACTED: Landslide susceptibility mapping at central Zab basin, Iran:
٤٤٠ A comparison between analytical hierarchy process, frequency ratio and logistic regression models. *CATENA, 115*, 55-
٤٤١ 70. doi:https://doi.org/10.1016/j.catena.2013.11.014
٤٤٢ Shirani, K., Pasandi, M., & Arabameri, A. (2018). Landslide susceptibility assessment by Dempster–Shafer and Index of Entropy
٤٤٣ models, Sarkhoun basin, Southwestern Iran. *Natural Hazards, 93*(3), 1379-1418. doi:10.1007/s11069-018-3356-2
٤٤٤ Sun, D., Wen, H., Wang, D., & Xu, J. (2020). A random forest model of landslide susceptibility mapping based on hyperparameter
٤٤٥ optimization using Bayes algorithm. *Geomorphology, 362*, 107201.
٤٤٦ doi:https://doi.org/10.1016/j.geomorph.2020.107201
٤٤٧ Thi Ngo, P. T., Panahi, M., Khosravi, K., Ghorbanzadeh, O., Kariminejad, N., Cerda, A., & Lee, S. (2021). Evaluation of deep learning
٤٤٨ algorithms for national scale landslide susceptibility mapping of Iran. Geoscience Frontiers, 12(2), 505-519.
٤٤٩ doi:https://doi.org/10.1016/j.gsf.2020.06.013
٤٥٠ Trang, N. T. Q., Ai, T. T. H., Giang, N. V., & Hoa, P. V. (2016). Object-based vs. pixel-based classification of mangrove forest mapping
٤٥١ in Vien An Dong Commune, Ngoc Hien District, Ca Mau Province using VNREDSat-1 images. Advances in Remote
٤٥٢ Sensing, 5(4), 284-295.
٤٥٣ Wang, L.-J., Guo, M., Sawada, K., Lin, J., & Zhang, J. (2016). A comparative study of landslide susceptibility maps using logistic
٤٥٤ regression, frequency ratio, decision tree, weights of evidence and artificial neural network. *Geosciences Journal, 20*(1),
٤٥٥ 117-136. doi:10.1007/s12303-015-0026-1
٤٥٦ Wang, Z., & Brenning, A. (2021). Active-Learning Approaches for Landslide Mapping Using Support Vector Machines. *Remote*
٤٥٧ *Sensing, 13*(13), 2588.
٤٥٨ Wei, C., Huang, Q., & Zhang, Y. (2008). *A new method to derive interval weights from an interval comparison matrix.* Paper
٤٥٩ presented at the 2008 7th World Congress on Intelligent Control and Automation.
٤٦٠ Xing, Y., Yue, J., Chen, C., Cai, D., Hu, J., & Xiang, Y. (2021). Prediction interval estimation of landslide displacement using adaptive
٤٦١ chicken swarm optimization-tuned support vector machines. *Applied Intelligence, 51*(11), 8466-8483.
٤٦٢ doi:10.1007/s10489-021-02337-y
٤٦٣ Zhang, Z., Yang, F., Chen, H., Wu, Y., Li, T., Li, W., . . . Liu, P. (2016). GIS-based landslide susceptibility analysis using frequency
٤٦٤ ratio and evidential belief function models. *Environmental Earth Sciences, 75*(11), 948. doi:10.1007/s12665-016-5732-
٤٦٥ 0
٤٦٦

Supplementary Files

This is a list of supplementary files associated with this preprint. Click to download.

- Declarations2.pdf